2011 11th IEEE-RAS International Conference on Humanoid Robots
Bled, Slovenia, October 26-28, 2011

Reactive Biped Walking Control for a Collision of a Swinging Foot on Uneven Terrain

Mitsuharu Morisawa, Fumio Kanehiro, Kenji Kaneko, Shuuji Kajita, and Kazuhiro Yokoi
Intelligent Systems Research Institute
National Institute of
Advanced Industrial Science and Technology (AIST)
Tsukuba Central 2, 1-1-1, Umezono, Tsukuba, Ibaraki 305-8568, Japan
Email: {m.morisawa, f-kanehiro, k.kaneko, s.kajita, Kazuhito.Yokoi}@aist.go.jp

***Abstract*—This paper describes a biped walking control method for a collision of a swinging foot on uneven terrain. Because a swing leg moves to a desired landing position, an unexpected collision on a terrain may be happened by a distance error between a foot and a terrain. A swing foot has to not only absorb a impact force, but also changes a trajectory as long as a swing foot contacts on a terrain. Furthermore it is required to keep a balance against a contact force. To prevent a trip over and a losing balance by contact on a terrain, two reactive key components are installed: 1) Set appropriate impedance gains of the feet according to a walking phase, 2) Update the desired landing position to the COG (Center of Gravity) pattern generation immediately as a detecting/releasing contact. In this paper, focused on a swing motion, a robust biped walking with a collision of a swinging foot on a uneven terrain is realized. The proposed method is validated through simulation results with the HRP-2 humanoid robot.**

I. INTRODUCTION

Biped locomotion can be achieved by switching a stance leg according to a reaction force from the ground alternately. Moving swing leg may contact on a terrain by a distance error between foot and terrain. When a collision between a swinging foot and a terrain is happened, what does a swing leg have to do ?

There are three types of contacts on a tarrain for a swinging foot during walking. Figure 1 (a) shows that a swinging foot is occurred an early contacts on a terrain for a preplanned landing at a early of single support phase (S.S.). In this case, a large horizontal impact force may act on a swinging foot and fall over halfway through a walking. Therefore it is necessary for a swing leg to absorb an unexpected contarct force. Moreover, a contact of a foot becomes physical constraints. As long as an unexpected collision is happened between a swinging foot and a terrain, it is also required to replan a trajectory of the foot. The other unexpected contacts of a swinging foot are at a late of landing just before and after a preplanned landing time in (b) and (c). In these cases, as soon as detecting a contact, a pattern generator stops the swing motion and a walking phase is switched from a single support phase to a double support phase immediately.

Several studys have been succeeded to walk on uneven terrain [1]-[6]. Yamaguchi was realized to walk on non-flat floor by using the sensors on the sole which measure a distance between a soleand a ground surface just before landing [1]. Mechanical foot system which adapts to a rough terrain was presented by Hashimoto [2]. Nishiwaki proposed a new framework of walking control system which updates the COG trajectory in a short cycle using the preview control, using the output the feedback controller that tracks the ZMP (Zero-Moment Point) reference [3] and a stratege for adjusting the ZMP reference by changing the next landing position and duration of the current step [4]. Takenaka proposes several balance control techniques which is to keep a ground reaction force [5]. In this method, as a result of the *model ZMP control* which accelerates the upper body, a landing position is modified locally.

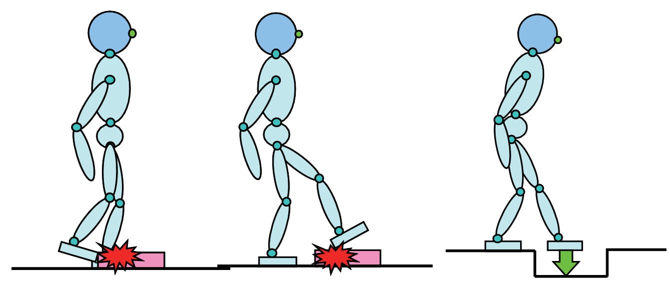

(a) early contact at a early of S.S. (b) early contact at a late of S.S. (c) late contact at a late of S.S.

Fig. 1. Unexpected contact for swing leg

However the most of researches are focused on a keeping a balance and supposed without a collision of a swing leg during walking. To prevent a trip over and a losing balance by contact on a terrain, we deal with a horizontal collision of a swinging foot during walking. The online generation method of a swing trajectory which updates an appropriate landing position sequentially is proposed. As a result of integrating between the online COG pattern generation and balance control via walking phase, a robust biped walking on a uneven terrain can be realized. The proposed method is validated through simulation results with the HRP-2 humanoid robot which walks on a rough terrain.

II. REACTIVE COG AND ZMP PATTERN GENERATION

We already proposed a new framework of the online COG and ZMP pattern generation which is composed of two terms [8]:

- Feed Forward term which generates the ideal COG and the ZMP trajectories from the previous and the future desired foot placements and its periods of the single/double support phases, and the COG and ZMP position and velocity at the beginning of the previous step. The future desired landing position and support periods can be changed at any time under the feedback term doesn't divergence. This term is permited to generate the discontinuous trajectories.
- Feedback term which is to track the ideal trajectories of the COG and the ZMP from the previous position and velocity of the COG and the ZMP. The role of this term is to guarantee a continuity of the COG and the ZMP trajectories within a support polygon.

In other words, the COG and the ZMP trajectories without the ZMP fluctuation can be defined as ideal trajectories. The difference between the current and ideal states are regarded as the errors that should be suppressed by a state-feedback controller.

The feed forward term as the ideal COG and ZMP is calculated by the analytical solution of the linear inverted pendulum with the piecewise ZMP polynomials which is formulated as

$$\boldsymbol{X}(T_{m+1}) = \boldsymbol{A}^{(m)}\boldsymbol{X}(T_1) + \boldsymbol{B}^{(m)}\boldsymbol{p} + \boldsymbol{C}^{(m)}\boldsymbol{a}, \quad (1)$$

where $\boldsymbol{A}^{(m)}$,$\boldsymbol{B}^{(m)}$ and $\boldsymbol{C}^{(m)}$ are constructed by the timings of the previous and the desired landing and $\boldsymbol{p}$ is the set of the previous and the future desired ZMP which corresponds to the previous and the future desired landing position. $\boldsymbol{a}$ is an unknown coefficient vector of from the forth-order ZMP polynomials. Substituting the COG states $\boldsymbol{X}(T_1)$ at the beginning of the previous step and the desired terminal states of the COG $\boldsymbol{X}(T_{m+1})$ which is supposed to stop after a few steps, the unknown coefficient vector $\boldsymbol{a}$ can be determined.

The feedback term as trajectory error compensation is generated by simulating an inverted pendulum with a state feedback control which is represented as follows.

$$\begin{aligned} \boldsymbol{x}^{err}(t+\Delta T) &= \boldsymbol{A}\boldsymbol{x}^{err}(t) + \boldsymbol{B}u(t) \quad (2) \\ u(t) &= -\boldsymbol{K}\boldsymbol{x}^{err}(t) \quad (3) \end{aligned}$$

$\boldsymbol{x}^{err} = [x^{err}\ \dot{x}^{err}\ p^{err}]^T$ are defined as the COG position and velocity and the ZMP position errors in x-axis which are acmount of the difference of the current and the previous ideal trajectories and the reduced value of the ZMP through a saturateion function Sat$(\cdot)$ by support polygon.

$$\begin{aligned} x^{err}(t) &\equiv x^{ideal}(t) - \mathcal{Z}^{-1}x^{ideal}(t-\Delta T), \quad (4) \\ p^{err}(t) &\equiv p^{ideal}(t) - \mathcal{Z}^{-1}p^{ideal}(t-\Delta T) \\ &\quad +\mathcal{Z}^{-1}\left(p^{ref}(t-\Delta T) - \text{Sat}\left(p^{ref}(t-\Delta T)\right)\right), \\ &\equiv p^{ideal}(t) - \mathcal{Z}^{-1}\bar{p}^{ref}(t-\Delta T) \quad (5) \end{aligned}$$

where $\bigcirc^{ideal}$ and $\bigcirc^{ref}$ denote the ideal trajectory and the reference trajectory which is added the feed forward term and the feedback term respectively. ΔT is a sampling preiod

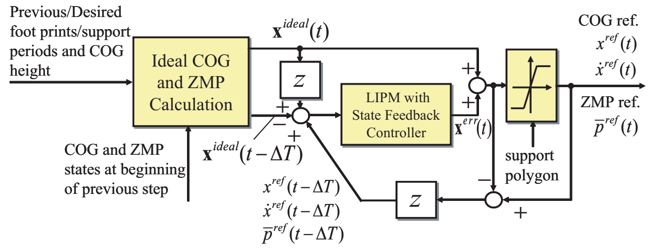

Fig. 2. Online COG and ZMP pattern generator

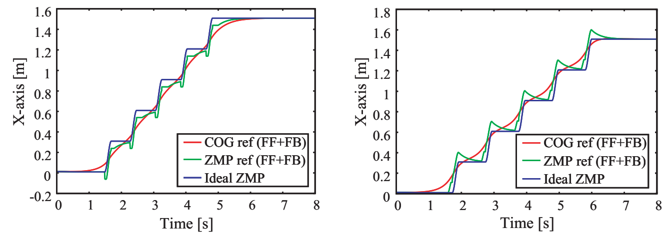

(a) In case of early landing (S.S. period 0.7s $\rightarrow$ 0.6s)

(b) In case of late landing (S.S. period 0.7s $\rightarrow$ 0.8s)

Fig. 3. COG and ZMP trajectories with early and late contact at late of S.S.

(= 5[ms]). $\mathcal{Z}$ is z transformation. The block diagram of this framework is shown in Fig. 2.

Figure 3 shows a comparison of the COG and the ZMP trajectories with an early and a late contacts at a late of single support phase. When a single support period is shorten from 0.7[s] to 0.6[s] with an early contact at 0.6[s] of S.S., the ZMP fluctuates backward to accelerate the COG (Fig. 3 (a)). On the contrary, when a single support period is extended from 0.7[s] until 0.8[s] with an late contact at 0.8[s], the ZMP fluctuates forward to decelerate the COG (Fig. 3 (b)). Through a saturation function for the ZMP reference, it can be strictly suppressed within a support polygon. We can see that the desired landing time can be increased and decreased just in landing. The feedback gains are calculated by the pole assignment :$\{-\omega, -\omega, -50\}$.

III. Foot motion generation

A rectangle trajectory of a foot can avoid a horizontal collision against a terrain which is lower height than the maximum swing height and can limit a contact force to a vertical direction. In contrast, a foot which is pursued a walking efficiency like a human becomes a likelihood of a collision on a terrain from a distance error between a swing leg and an environment. In order to provide a walking performance or reduce a feeling of strangeness during walking, it should not introduce a limitation of a swing trajectory. In return for this limitation, it is necessary to prepare for a collision of a swing leg with a terrain.

A. coordinate system

There are two roles of a swing leg motion: one is to move the desired landing position. The other is the control of a

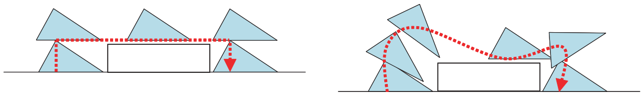

(a) rectangle trajectory (more safety)

(b) human like trajectory (more efficiency)

Fig. 4. Swing leg trajectories : (a) Rectangle trajectory becomes more safety which lifts up and touches down a foot vertically, (b) Human like trajectory is expected to walk effiently in term of walking speed, energy and joint torque.

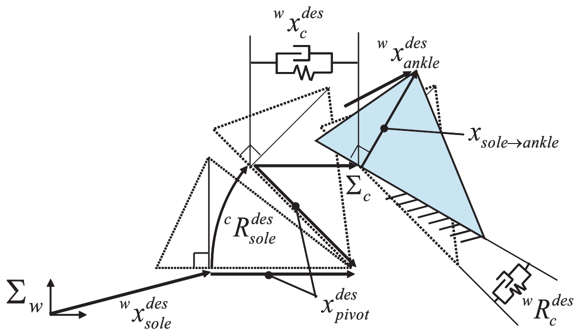

- ${}^{w}\boldsymbol{x}_{sole}^{des}(t)$: Desired sole position vector which is defined on the bottom of an ankle without rolling in the world coordinates $\sum_w$
- $\boldsymbol{x}_{pivot}^{des}(t)$: Desired pivot position vector from the desired sole position to a center of the foot rolling
- ${}^{w}\boldsymbol{x}_c^{des}(t)$: Relative position vector which denotes a displacement through the foot force control in $\sum_w$
- ${}^{c}\boldsymbol{R}_{sole}^{des}(t)$: Desired sole attitude matrix which is for a rolling motion of the foot
- ${}^{w}\boldsymbol{R}_c^{des}(t)$: Sole attitude matrix which is generated by the foot torque controller

Fig. 5. Coordinate system of foot

contact force and torque in order to keep a balance at the support phase and absorb a contact force from a swing leg. Because the degree of freedom of the legs is changed with a contact states of the feet, the desired translate and rotate trajectories of the feet are represented as a time function analytically. All of feet trajectories are generated sequentially at every sampling period from the current value. Then the desired ankle position can be calculated by these trajectories and the desired joint angles of the legs can be converted from the position and the attitude of waist and ankles by the inverse kinematics. The coordinate system of the foot is shown in Fig. 5. The foot motion is generated by synthesis of the desired translate and rotate trajectories of the foot ${}^{w}\boldsymbol{x}_{sole}^{des}(t)$ and ${}^{c}\boldsymbol{R}_{sole}^{des}(t)$, the relative position from the origin of the foot force control to a center of foot ration $\boldsymbol{x}_{pivot}^{des}(t)$, and the output position and attitude by the foot force control ${}^{w}\boldsymbol{x}_c^{des}(t)$ and ${}^{w}\boldsymbol{R}_c^{des}(t)$. Then the desired ankle position and attitude can be obtained.

$$\begin{aligned} {}^{w}\boldsymbol{x}_{ankle}^{des} &= {}^{w}\boldsymbol{x}_{sole}^{des} + {}^{w}\boldsymbol{R}_c^{des}(\boldsymbol{x}_{pivot}^{des} - {}^{c}\boldsymbol{R}_{sole}^{des}\boldsymbol{x}_{pivot}^{des}) \\ &+ {}^{w}\boldsymbol{x}_c^{des} + {}^{w}\boldsymbol{R}_c^{des}\cdot{}^{c}\boldsymbol{R}_{sole}^{des}\boldsymbol{x}_{sole\to ankle} \qquad (6) \\ {}^{w}\boldsymbol{R}_{ankle}^{des} &= {}^{w}\boldsymbol{R}_c^{des}\cdot{}^{c}\boldsymbol{R}_{sole}^{des} \qquad (7) \end{aligned}$$

B. desired horizontal trajectory

The desired horizontal trajectory of the sole is generated by connecting from the current position and velocity to the desired landing position sequentially. First we suppose a virtual motion equation of a sole which can be expressed as follows:

$$\dot{\boldsymbol{x}} = \boldsymbol{A}\boldsymbol{x} + \boldsymbol{B}u, \qquad (8)$$

where

$$\boldsymbol{A} = \begin{bmatrix} 0 & 1 \\ 0 & 0 \end{bmatrix}, \boldsymbol{B} = \begin{bmatrix} 0 \\ 1 \end{bmatrix}, \qquad (9)$$

$\boldsymbol{x} = [x\ \dot{x}]^T$ is a state vector and u is virtual input. x denotes a horizontal position of the sole in x-axis. The desired sole trajectory in y-axis is also generated by the same approach. The optimal trajectoy can be obtained as a solution of two-point boundary value problem. The cost function J is set as follows:

$$J = \int_{t_0}^{t_1} \boldsymbol{x}^T\boldsymbol{Q}\boldsymbol{x} + ru^2 dt, \qquad (10)$$

where $\boldsymbol{Q} = \mathrm{diag}\{q_1, q_2\}$ and r are weight matrix and value respectively. t_0 and t_1 are current and terminal time for the horizontal motion. To prevent a large velocity of the sole, let us consider the minimum solution of square sum of velocity. Thus, weight matrix and value become $q_1 = 0, q_2 = 1, r = 1$. The general solution can be derived through *Hamilton-Jacobi* equation.

$$x(t) = C_1^h e^t + C_2^h e^{-t} + C_2^h t + C_4^h \qquad (11)$$

The coefficients of $C_i^h (i = 1\ldots4)$ in (11) are determined from the boundary conditions, that is the current and the terminal position and velocity: $x(t_0), \dot{x}(t_0), x(t_1), \dot{x}(t_1)$.

When a swinging foot contacts on a terrain, it is necessary to stop immediately. As long as the foot detects a collision, a velocity of the swinging foot decelerates exponentially.

$$\dot{x}(t) = C_1^s e^t + C_2^s \qquad (12)$$

Integrating (12), the deceleration trajectory can be represented as follows:

$$x(t) = C_1^s e^t + C_2^s t + C_2^s \qquad (13)$$

From the current position and velocity $x(t_0), \dot{x}(t_0)$ and the terminal velocity condition $\dot{x}(t_{stop}) = 0$, the coefficients of (13) can be calculated. The stop time $t_{stop}(= 0.05[s])$ is prepared to avoid a limit over of a joint torque. When the foot is released from the collision, it is expected to approach for a swinging foot to the original desired landing position as possible. Therefore, the desired landing position x_{land}^{des} is recalculated so that the average velocity of the swinging foot can satisfy a velocity limit v_{lim}.

$$ {}^{w}x_{sole}^{des} = \begin{cases} \text{if } \left|\frac{x_{land}^{des}-x_{cur}}{T_{land}-T_{cur}}\right| <= v_{lim} & : x_{land} \\ \text{else} & : x_{cur}+v_{lim}(T_{land}-T_{cur}) \end{cases} \quad (14) $$

Where x_{cur} is the current sole position and T_{land}, T_{cur} are the desired landing and the current time respectively. In addition to the velocity condition in (14), the balance condition of the COG and the ZMP must be taken into account.

C. desired vertical trajectory

When a robot walks on uneven terrain, the swing leg may land on a ground earlier or later than the preplanned time. The difference between an actual and a desired landing time is easily to lose a balance. Force control between a foot and a ground will reduce an influence of impact force by early contact. In case of late contact, the ZMP is desired to keep on a foot. In terms of the ZMP and the COG trajectory errors, the swing leg is expected to land on a ground as soon as possible. Therefore, a period of the constant velocity in vertical direction is introduced before landing. The same approach is shown in [9]. The desired vertical trajectory is generated by fifth-order time polynomial.

A period of the current single support phase T_{ss} can be shorten or extended according to the detection of a vertical contact force. If a contact force is not detected until the preplanned landing time, a period of the current single support phase is increased by sampling period ($\Delta T = 5$[ms]).

$$ T_{ss} = \begin{cases} \text{if } T_{land} \geq T_{contact} & : T_{ss} - (T_{land} - T_{contact}) \\ \text{else } T_{land} < T_{contact} & : T_{ss} + \Delta T \end{cases} \quad (15) $$

Where, $T_{contact}$ and T_{land} are the time when a contact force is detected and the desired landing time respectively. Then the single support is switched to the double support phase immediately after a contact force detection. Here we consider a rotation of the swinging foot. In order to shift the weight of the body smoothly, the beginning and the end of the foot rolling is set at a half of the double support phase. When a swinging foot contacts on a ground, the foot still rotates around the heel. Early contact may request a large angular velocity of the foot. Therefore regardless of contact time, duration of the foot rolling is kept by changing a duration of next double support phase T_{ds}.

$$ T_{ds} = \begin{cases} \text{if } T_{contact} \geq T_{land} & : T_{ds} \\ \text{else} & : 2(T_{land} - T_{contact}) \end{cases} \quad (16) $$

D. desired rolling trajectory

A foot rolling is realized by a pivot vector and a rotation around the pivot. The pivot vector which denotes a center of rolling is introduced for a foot rolling motion around toe or heel. When a robot walks forward, the pivot vector points to its toe. On contrary, when a foot touches down on a ground, the pivot vector points to its heel. During a swing leg, the pivot vector moves from a toe to a heel. The trajectory of the pivot vector is generated as well as the horizontal trajectory of the sole in (11). For the foot rolling, two intermediate points are also interpolated by fifth order time polynomial. The time chart for the swing leg is shown in Fig.6.

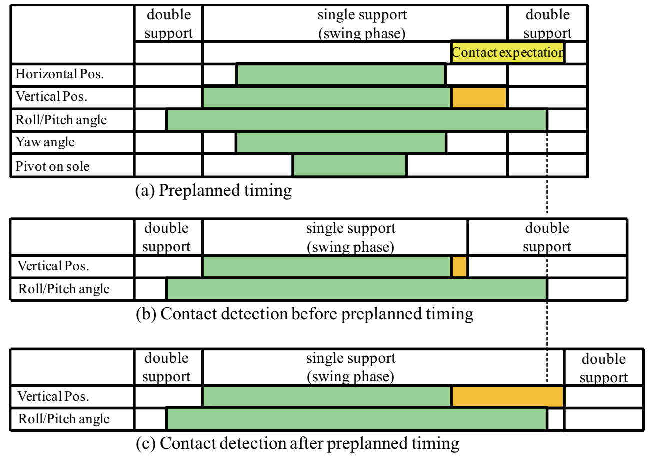

Fig. 6. Timing of swing leg position and attitude

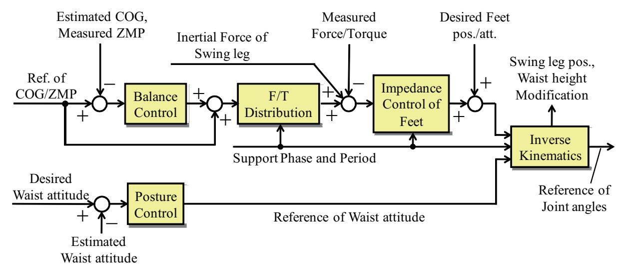

Fig. 7. Overview of control system

IV. CONTACT FORCE CONTROL

A. force/torque control

An overview of stabilization control structure proposed by Kajita [6] is shown in Fig. 7. The feet are controlled to follow the desired force and torque reference from the balance controller. The foot force controller is implemented as an admittance control.

$$ \boldsymbol{M} {}^{w}\ddot{\boldsymbol{x}}_c^{des} + \boldsymbol{D}_T {}^{w}\dot{\boldsymbol{x}}_c^{des} + \boldsymbol{K}_T {}^{w}\boldsymbol{x}_c^{des} = \boldsymbol{K}_f(\boldsymbol{F}^{ref} - \boldsymbol{F}^{res}) \quad (17) $$

Where $\boldsymbol{M}$,$\boldsymbol{D}_T$ and $\boldsymbol{K}_T$ are matrices of mass, damping and stiffness for a translational impedance model respectively. $\boldsymbol{K}_f$ is force gain which is set to zero to block an external force at the single support phase. $\boldsymbol{F}^{ref}$ and $\boldsymbol{F}^{res}$ are the reference and the measured force vector.

The foot torque controller modifies foot rotation to realize the foot reference torque calculated by the ZMP distributor. We use the following damping controller to realize given foot torque $\boldsymbol{\tau}^{ref}$.

$$ \boldsymbol{D}_R \dot{\delta}^{des} + \boldsymbol{K}_R \delta^{des} = \boldsymbol{K}_m(\boldsymbol{\tau}^{ref} - \boldsymbol{\tau}^{res}) \quad (18) $$

where $\boldsymbol{D}_R$ and $\boldsymbol{K}_R$ are damping and stiffness gain concerned with a rolling of the sole. Let us define a function damping()

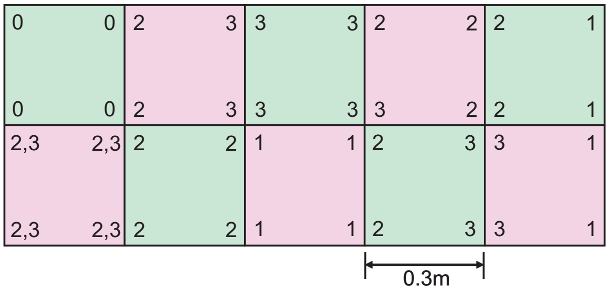

Fig. 8. Height of uneven terrain [cm] (top view)

which returns a control variable δ^{des} for the given torque measurement and reference by (18). The foot reference frame is modified to control x and y component of the foot torque.

$$
\begin{aligned}
{}^{w}\boldsymbol{R}_{c,i}^{des} &= \boldsymbol{RPY}(\Delta\phi, \Delta\theta, 0)(i = R, L) && (19)\\
\Delta\phi_i &= \text{damping}(\tau_{ix}^{ref}, \tau_{iy}^{ref}) && (20)\\
\Delta\theta_i &= \text{damping}(\tau_{ix}^{ref}, \tau_{iy}^{ref}) && (21)
\end{aligned}
$$

B. collision detection

To prevent a chattering motion of a swing leg, the collision in a horizontal direction is detected through an admittance control.

$$
\begin{array}{ll}
\text{if } \ |x_c^{des}| \geq x_{contact} & : \text{contact in } x\text{-axis} \\
\text{else} & : \text{non-contact in } x\text{-axis}
\end{array} \quad (22)
$$

The collision detection in y-axis is also same way as in x-axis. In case of the vertical direction, the collision is detected by the measurement vertical force.

$$
\begin{array}{ll}
\text{if } \ F_z^{res} \geq F_{z\,contact} & : \text{contact} \\
\text{else} & : \text{non-contact}
\end{array} \quad (23)
$$

V. Simulation Results

For general discussion, an arbitrary unevern terrain is prepared. Any information about terrain such as the location, the height, and the inclination is not provided for the walking control. The height of uneven terrain is shown in a corner of the square terrain in Fig. 8. In order to assure a collision of the foot on uneven, the foot lands closer to the uneven terrain at first step. The step length of first and second steps are 0.25[m] and others are 0.3[m]. The desired walking cycle is 0.9[s]. Two types of the height (2cm, 3cm) on the first uneven (left bottom) are tested.

Figure 11 shows the snapshot of walking with a collision of a swinging foot on uneven floor. The height of the first uneven (at the lower left of Fig. 8) is set to 2cm. The second step of the right foot hit on a uneven at early period of the single support phase. Because the swing velocity of the foot is not so fast at the beginning of the single support phase, the impact force could be absorbed by force control on horizontal plane. However, unless the foot trajectory is changed after collision, the foot will manage to push an uneven and then the robot will fall down. In proposed method, the stable walking could be realized by collaborating the reactive COG and ZMP pattern generation and the horizontal force control on the swing leg. In Fig. 9, we can see that the COG and the ZMP was controlled stably during walking. In case of 2cm height of first terrain, the foot detected on a contact at 6.4[s]. Shortly after the contact, it was released and the foot tried to land closer to the desired landing position under the swing velocity limitation. In case of 3cm, because it was not released after the first contact, the landing position became almost the initial position (Fig. 10). The snapshot for a comparison of the swing leg trajectories with 2cm and 3cm height of first uneven is shown in Fig. 12.

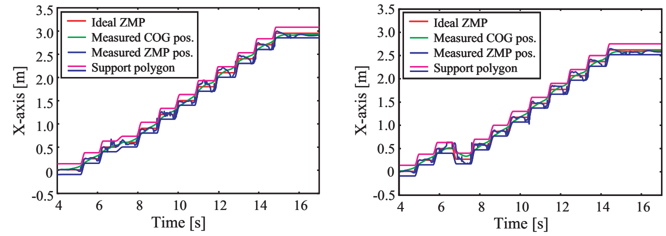

(a) 2cm height on first terrain

(b) 3cm height on first terrain

Fig. 9. COG and ZMP responses in x-axis

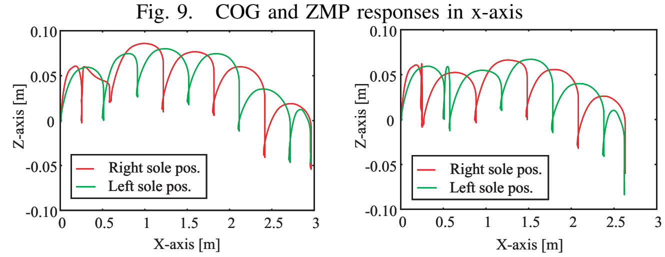

(a) 2cm height on first terrain

(b) 3cm height on first terrain

Fig. 10. Sole trajectories with collision in x-z plane

VI. Conclusion

In this paper, the collaboration between the reactive pattern generation of the COG and ZMP and a swing motion, could be realized a robust biped walking on a uneven terrain. To escape a trip over and a losing balance by contact on a terrain, how to update pattern generation immediately as detecting contact on a terrain, and how to modify a swing leg trajectory from a collision force were proposed. The proposed method was validated through simulation results with the HRP-2 humanoid robot. To investigate a feasibility for a collision of a swinging foot at the whole period of the single support phase is our future work.

Acknowledgment

Authors would like to thank Koichi Nishiwaki and Satoshi Kagami of Digital Human Research Center, and Nobuyuki Kita, Shin'ichiro Nakaoka, and Kanako Miura of Humanoid Research Group AIST for their useful advices.

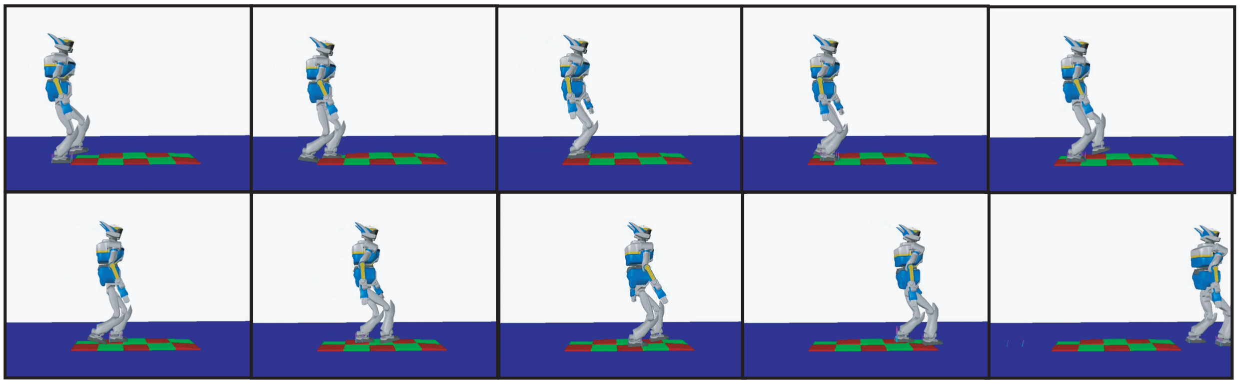

Fig. 11. Snapshot of walking simulation (first terrain = 2cm)

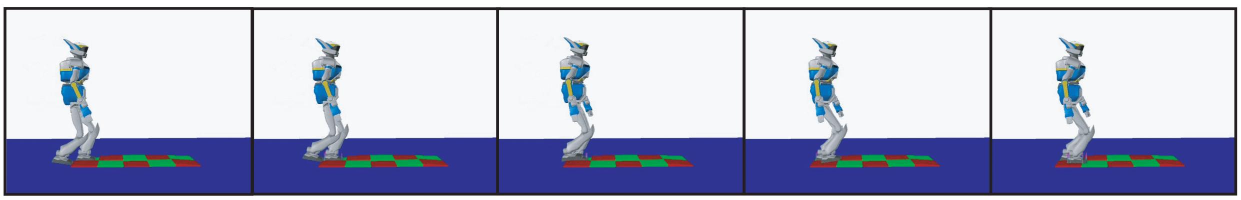

(a) 2cm height on first terrain

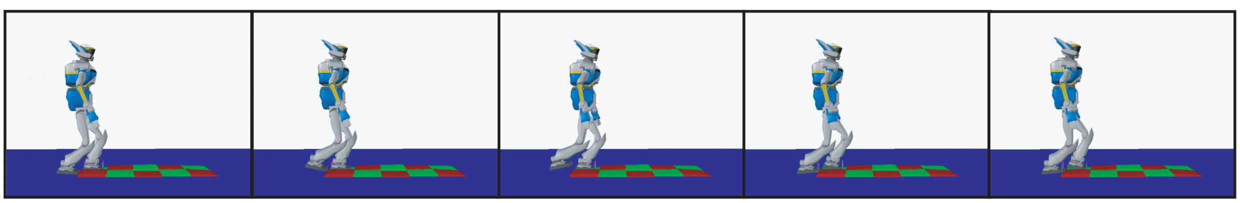

(b) 3cm height on first terrain

Fig. 12. Comparison of swing behavor with collision

REFERENCES

[1] J. Yamaguchi, A. Takanishi and I. Kato, "Development of a Biped Walking Robot Adapting to a Horizontally Uneven Surface," *Proc. of IEEE/RSJ Int. Conf. on Intelligent Robots and Systems (IROS'94)*, pp.1156-1163, 1994.

[2] K. Hashimoto, Y. Sugahara, M. Kawase, A. Ohta, C. Tanaka, A. Hayashi, N. Endo, T. Sawato, H. Lim, and A. Takanishi, "Landing Pattern Modification Method with Predictive Attitude and Compliant Control to Deal with Uneven Terrain," *in Proc. of IEEE/RSJ Int. Conf. on Intelligent Robotics and Systems (IROS'06)*, pp.1755-1760, 2006.

[3] K. Nishiwaki, and S. Kagami, "High Frequency Walking Pattern Generation based on Preview Control of ZMP," *in Proc. of IEEE Int. Conf. on Robotics and Automation*, pp.2667-2672, 2006.

[4] K. Nishiwaki, and S. Kagami, "Strategies for Adjusting the ZMP Reference Trajectory for Maintaining Balance in Humanoid Walking," *in Proc. of IEEE Int. Conf. on Robotics and Automation*, pp.4230-4236, 2010.

[5] T. Takenaka, T. Matsumoto, T. Yoshiike, T. Hasegawa, S. Shirokura, H. Kaneko and A. Orita, "Real Time Motion Generation and Control for Biped Robot -4th Report: Integrated Balance Control-," *in Proc. of IEEE/RSJ Int. Conf. on Intelligent Robots and Systems (IROS'09)*, pp.1601-1608, 2009.

[6] S. Kajita, M. Morisawa, K. Miura, S. Nakaoka, K. Harada, K. Kaneko, F. Kanehiro, K. Yokoi, "Biped walking stabilization based on linear inverted pendulum tracking," *in Proc. of IEEE/RSJ Int. Conf. on Intelligent Robots and Systems*, pp.4489-4496, 2010.

[7] M. Morisawa, K. Harada, S. Kajita, K. Kaneko, J. Sola, E. Yoshida, N. Mansard, K. Yokoi, J-P. Laumond, "Reactive stepping to prevent falling for humanoid robots," *in Proc. of IEEE Int. Conf. on Humanoids*, pp.528-534, 2009.

[8] M. Morisawa, F. Kanehiro, K. Kaneko, N. Mansard, J. Sola, E. Yoshida, K. Yokoi, and J-P. Laumond, "Combining Suppression of the Disturbance and Reactive Stepping for Recovering Balance," *in Proc. of IEEE Int. Conf. on Intelligent Robots and Systems (IROS)*, pp.3150-3156, 2010.

[9] K. Nishiwaki, and S. Kagami, "Frequent Walking Pattern Generation that Uses Estimated Actual Posture for Robust Walking Control," *in Proc. of IEEE-RAS Int. Conf. on Humanoid Robots*, pp.535-541, 2009.

[10] T. Sugihara, and Y. Nakamura, "Contact Phase Invariant Control for Humanoid Robot based on Variable Impedant Invaerted Pendulum Model," in Proc. of IEEE Int. Conf. on Robotics and Automation, pp.51-56, 2003.

[11] S. Hong, Y. Oh, Y. H. Chang, and B. J. You, "An Omni-directional Walking Pattern Generator Method for Humanoid Robots with Quartic Polynomials," *in Proc. of IEEE/RSJ Int. Conf. on Intelligent Robots and Systems*, pp.4207-4213, 2007.

[12] F. Kanehiro, W. Suleiman, K. Miura, M. Morisawa, E. Yoshida, "Feasible pattern generation method for humanoid robots," *in Proc. of IEEE-RAS Int. Conf. Humanoid Robots*, pp.542-548, 2009.

[13] F. Kanehiro, M. Morisawa, W. Suleiman, K. Kaneko, E. Yoshida, "Integrating geometric constraints into reactive leg motion generation," *in Proc of IEEE/RSK Int. Conf. on Intelligent Robots and Systems* (IROS), pp.4069-4076, 2010.